

# High-Density Lipoprotein Nanobiologics for Precision Medicine

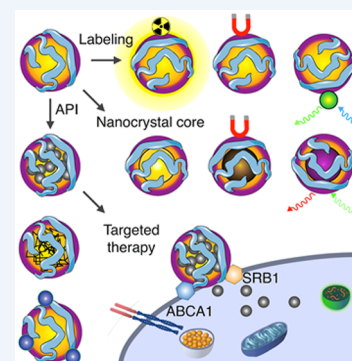
Willem J. M. Mulder,<sup>\*,†,‡,§</sup> Mandy M. T. van Leent,<sup>†,‡</sup> Marnix Lameijer,<sup>‡</sup> Edward A. Fisher,<sup>§</sup> Zahi A. Fayad,<sup>†</sup> and Carlos Pérez-Medina<sup>\*,†</sup>

<sup>†</sup>Translational and Molecular Imaging Institute, Icahn School of Medicine at Mount Sinai, New York, New York 10029, United States

<sup>‡</sup>Department of Medical Biochemistry, Academic Medical Center, 1105 AZ Amsterdam, The Netherlands

<sup>§</sup>Department of Medicine (Cardiology) and Cell Biology, Marc and Ruti Bell Program in Vascular Biology, NYU School of Medicine, New York, New York 10016, United States

**CONSPECTUS:** Nature is an inspirational source for biomedical engineering developments. Particularly, numerous nanotechnological approaches have been derived from biological concepts. For example, among many different biological nanosized materials, viruses have been extensively studied and utilized, while exosome research has gained much traction in the 21st century. In our body, fat is transported by lipoproteins, intriguing supramolecular nanostructures that have important roles in cell function, lipid metabolism, and disease. Lipoproteins' main constituents are phospholipids and apolipoproteins, forming a corona that encloses a hydrophobic core of triglycerides and cholesterol esters. Within the lipoprotein family, high-density lipoprotein (HDL), primarily composed of apolipoprotein A1 (apoA-I) and phospholipids, measuring a mere 10 nm, is the smallest and densest particle. Its endogenous character makes HDL particularly suitable as a nanocarrier platform to target a range of inflammatory diseases.



For a decade and a half, our laboratories have focused on HDL's exploitation, repurposing, and reengineering for diagnostic and therapeutic applications, generating versatile hybrid nanomaterials, referred to as nanobiologics, that are inherently biocompatible and biodegradable, efficiently cross different biological barriers, and intrinsically interact with immune cells. The latter is facilitated by HDL's intrinsic ability to interact with the ATP-binding cassette receptor A1 (ABCA1) and ABCG1, as well as scavenger receptor type B1 (SR-BI). In this Account, we will provide an up-to-date overview on the available methods for extraction, isolation, and purification of apoA-I from native HDL, as well as its recombinant production. ApoA-I's subsequent use for the reconstitution of HDL (rHDL) and other HDL-derived nanobiologics, including innovative microfluidic-based production methods, and their characterization will be discussed. The integration of different hydrophobic and amphiphilic imaging labels, including chelated radioisotopes and paramagnetic or fluorescent lipids, renders HDL nanobiologics suitable for diagnostic purposes. Nanoengineering also allows HDL reconstitution with core payloads, such as diagnostically active nanocrystals, as well as hydrophobic drugs or controlled release polymers for therapeutic purposes. The platform technology's specificity for inflammatory myeloid cells and methods to modulate specificity will be highlighted. This Account will build toward examples of *in vivo* studies in cardiovascular disease and cancer models, including diagnostic studies by magnetic resonance imaging (MRI), computed tomography (CT), and positron emission tomography (PET). A translational success story about the escalation of zirconium-89 radiolabeled HDL (<sup>89</sup>Zr-HDL) PET imaging from atherosclerotic mice to rabbits and pigs and all the way to cardiovascular disease patients is highlighted. Finally, recent advances in nanobiologic-facilitated immunotherapy of inflammation are spotlighted. Lessons, success stories, and perspectives on the use of these nature-inspired HDL mimetics are an integral part of this Account.

## 1. INTRODUCTION

Nature is an inspirational source for biomedical engineering developments. Particularly, numerous nanotechnological approaches have been derived from biological concepts.<sup>1</sup> In our body, fat is transported by lipoproteins, fascinating supramolecular nanostructures that have important roles in cell function, lipid metabolism, and disease progression. Lipoproteins' main constituents are phospholipids and apolipoproteins, forming a corona that encloses a hydrophobic core of triglycerides and cholesterol esters.<sup>2</sup> Their endogenous character makes lipoproteins particularly suitable as nanocarriers for diagnostic or therapeutic agents, rendering versatile

hybrid materials that are inherently biocompatible and biodegradable and efficiently cross different biological barriers.

Measuring a mere 10 nm in diameter, high-density lipoprotein (HDL), primarily composed of apolipoprotein A1 (apoA-I) and phospholipids, is the smallest and densest (hence its name) particle in the lipoprotein family.<sup>3</sup> Contrary to larger lipoproteins' delivery function, HDL particles remove cellular fat molecules for transportation back to the liver, from which apoA-I originates.<sup>4</sup> For a decade and a half, our laboratories and others have focused on HDL's exploitation, repurposing, and

Received: August 15, 2017

Published: December 27, 2017

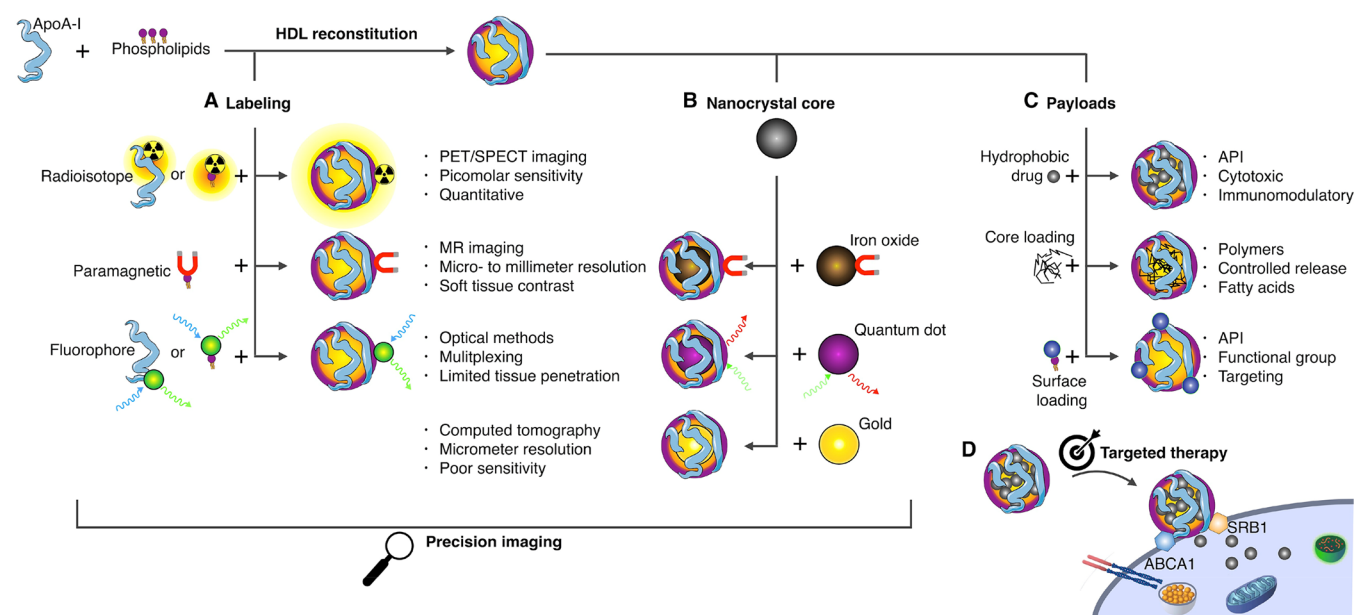


**Figure 1.** HDL nanobiologic platform technology. HDL is reconstituted from apolipoprotein A1 (apoA-I) and phospholipids. The HDL scaffold can be customized to include (A) amphiphilic or lipophilic imaging labels or (B) a diagnostically active nanocrystal core, rendering HDL nanobiologics suitable for precision and molecular imaging purposes. In addition, these labeling strategies can be deployed to understand HDL nanobiologics *in vitro* and *in vivo* behavior, with optical methods, nuclear imaging, as well as CT and MRI. (C) Payloads for therapeutic purposes can be incorporated in HDL nanobiologics. (D) HDL nanobiologics engage immune cells through apoA-I's binding capacity for the adenosine triphosphate-binding cassette transporter A1 (ABCA1) and the scavenger receptor type B-1 (SR-B1).

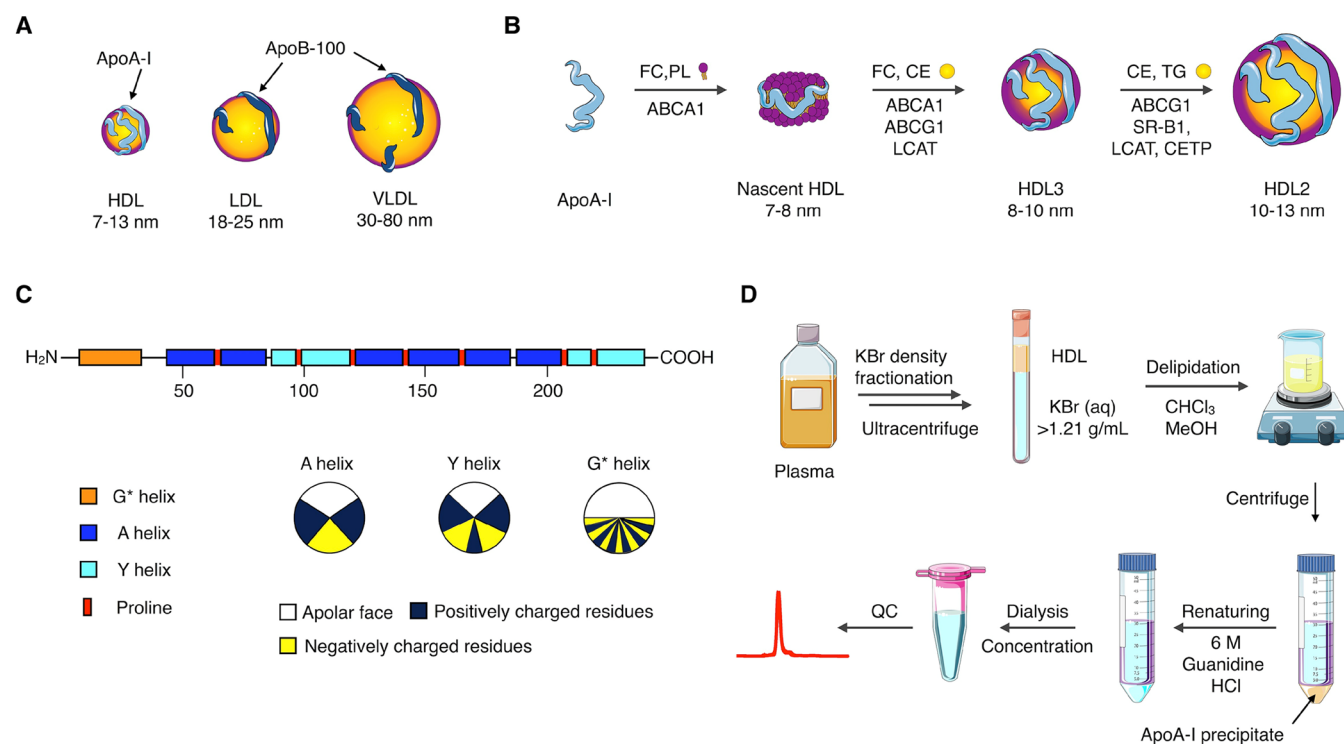


**Figure 2.** HDL/apoA-I properties, function, and production. (A) HDL is the smallest and densest member of the lipoprotein family. (B) Maturation process of native HDL. (C) Schematic representation of apoA-I's primary structure, showing the different  $\alpha$ -helix domains. The amphipathic helix classes are shown below.<sup>2</sup> (D) Isolation of apoA-I from blood plasma.

reengineering for diagnostic and therapeutic applications in cardiovascular diseases and cancer, two of the leading causes of mortality and morbidity worldwide.

We will provide an up-to-date overview on the isolation, purification, characterization, and component extraction of

native HDL. Innovative production and reconstitution methods<sup>5,6</sup> are a special emphasis of this Account. The integration of different amphiphilic imaging labels, including chelated radioisotopes<sup>7,8</sup> or paramagnetic and fluorescent lipids,<sup>9,10</sup> renders so-called HDL nanobiologics suitable for

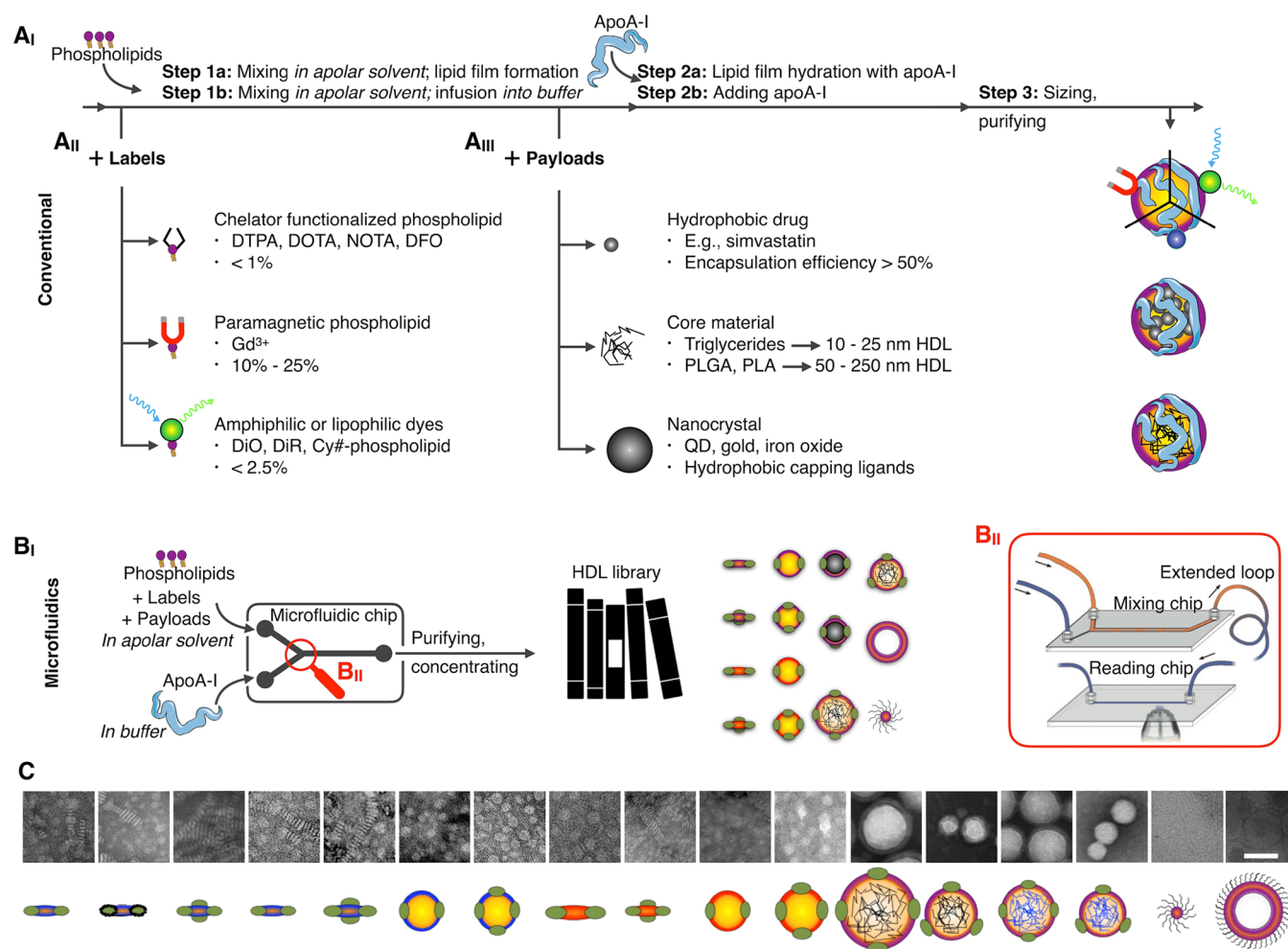


**Figure 3.** HDL nanobiologics production. (A<sub>I</sub>) HDL can be reconstituted per different “conventional” strategies and include (A<sub>II</sub>) amphiphilic labels or (A<sub>III</sub>) hydrophobic core payloads. (B<sub>I</sub>) Microfluidic technology allows HDL nanobiologic instantaneous formation, (B<sub>II</sub>) a process that can be monitored by FRET confocal microscopy (reproduced with permission from ref 24; copyright 2017 Wiley). Judicious control over solvents, reagent concentration, infusion speeds, and microfluidic chip design facilitates establishing nanobiologic libraries. (C) Transmission electron micrographs (scale bar 50 nm) and schematic representations of HDL nanobiologic library. Adapted with permission from ref 15. Copyright 2016 National Academy of Sciences of the United States of America.

diagnostic purposes (Figure 1A). Nanoengineering also allows HDL reconstitution with core payloads, such as diagnostically active nanocrystals<sup>11–13</sup> (Figure 1B), as well as hydrophobic drugs<sup>14,15</sup> or controlled-release polymers<sup>6,15</sup> (Figure 1C) for therapeutic purposes. The latter can also be achieved by the inclusion of therapeutically active surface payloads. Modification and hybridization of HDL nanobiologics for diagnostic and therapeutic objectives will be thoroughly discussed. The platform technology’s specificity for inflammatory myeloid cells (Figure 1D) and methods to modulate specificity will be highlighted.

This Account will build toward examples of diagnostic studies in animal disease models and human subjects by magnetic resonance imaging (MRI), computed tomography (CT), and positron emission tomography (PET). Finally, recent advances in nanobiologic-facilitated immunotherapy of inflammation are spotlighted.

## 2. HDL PROPERTIES AND ISOLATION

### 2.1. HDL’s Structure and Function

HDL is the smallest of the lipoprotein family<sup>16</sup> (Figure 2A, chylomicrons, not shown, range from 75 nm to 1.2 μm). Its main protein component, apoA-I,<sup>17</sup> is produced in the liver and intestines and progressively takes up phospholipids and free cholesterol (FC) through interaction with ATP-binding cassette receptor A1 (ABCA1) to give rise to discoidal nascent HDL.<sup>16</sup> Subsequent interaction with ABCA1 and ABCG1 leads to increased cholesterol content, which is esterified by lecithin-cholesterol acyl transferase (LCAT), an enzyme that is activated by apoA-I (Figure 2B). The resulting hydrophobic cholesteryl esters (CE) move to the core of the particle, thus causing a shape change from discoidal to spherical. Mature HDL nanoparticles are the result of further uptake of free cholesterol, through ABCG1 and scavenger receptor type B1 (SR-B1), CEs, through esterification by LCAT, and triglycerides (TGs), through a CE/TG exchange with other lipoproteins catalyzed by the “on-board” enzyme cholesteryl ester transfer protein (CETP).<sup>16</sup> HDL is therefore a dynamic nanoparticle system, in terms of size (ranging from 7 to 13 nm in diameter

and 170 to 360 kDa in mass), shape, and composition. The collected cholesterol from peripheral tissues is then carried to the liver for excretion in a process termed reverse cholesterol transport (RCT). Indeed, RCT is one of the main physiological roles of HDL and the mechanism whereby it is believed to exert its atheroprotective effects. ApoA-I and HDL, however, possess a plethora of other antioxidant and anti-inflammatory properties. The natural affinity of apoA-I for the above-mentioned receptors lend HDL nanoparticles an inherent targeting ability. These receptors are abundantly expressed by myeloid cells, thus making HDL an ideal platform for precision medicine targeting these cell populations, which are key players in inflammatory disorders.

## 2.2. ApoA-I Production

ApoA-I is a 28.1 kDa protein that contains 10 amphipathic  $\alpha$ -helical regions, making up to approximately 80% of the total 243 amino acids<sup>2</sup> (Figure 2C). These regions vary in the distribution of positively and negatively charged residues around the helix axis and have a nonpolar face of variable hydrophobicity and lipid binding affinity. While HDL nanobiologics can be prepared by direct use of native nanoparticles isolated from plasma, this can be problematic due to difficult modification (loading) and, especially, safety. For this reason, reconstituted HDL (rHDL) nanoparticles are greatly preferred. In this process, the HDL components, typically apoA-I and phospholipids, are added separately, and a process of self-assembly, sometimes aided by sonication or microfluidics, generates the nanoparticles. Although both building blocks are commercially available, apoA-I is expensive and it is usually obtained through extraction from blood/plasma (Figure 2D), especially when required in large quantities. The separation process is laborious and includes several centrifugation-based density fractionation steps to first isolate HDL (density 1.07–1.20 g/mL). Delipidation of HDL nanoparticles with organic solvents leads to precipitation of lipid-poor apoA-I that needs to be renatured using 6 M guanidine hydrochloride. Finally, dialysis against the desired buffer yields apoA-I with purities typically higher than 90%, as determined by gel electrophoresis or size exclusion chromatography (SEC). There are, however, challenges associated with this procedure due to the large volumes of organic solvents required and the potential presence of pathogens in the blood/plasma of origin.

## 2.3. ApoA-I Mimetics and Recombinant Production of apoA-I

Alternatively, small oligopeptides with similar lipid binding properties to apoA-I can be used to prepare rHDL nanoparticles.<sup>18</sup> These peptides contain typically fewer than 40 amino acids, and the nanoparticles generated from them retain the ability to efflux cholesterol from loaded macrophages. One of the main advantages of using apoA-I mimetics is the reduced cost compared to the whole protein. Finally, apoA-I can also be produced using recombinant DNA expressed in *E. coli*<sup>19</sup> or mammalian cells.<sup>20</sup> This approach is not completely devoid of challenges, as purification of the recombinant protein is difficult and yields are generally low.

## 3. PRODUCTION OF HDL NANOBIOLOGICS

The ability to design and produce HDL-mimicking nanobiologics relies primarily on apoA-I's unique properties. As described in the previous section, apoA-I is an amphipathic helical protein that contains polar and nonpolar faces along its long axis.<sup>2</sup> This enables its exploitation as building block for

supramolecular self-assembled phospholipid aggregates, where apoA-I serves as a structural stabilizer of small bilayered discs. The inclusion of lipophilic payloads forces discoidal HDL to become spherical, in which a phospholipid monolayer, with apoA-I embedded, encloses a hydrophobic core of, for example, triglycerides, in essence forming an emulsion. HDL's structural properties and its individual building block features provide a framework for the design and production of HDL-mimicking and HDL-derived hybrid nanobiologics.

### 3.1. Conventional Methods

HDL reconstitution<sup>16</sup> is traditionally achieved by (i) the formation of bilayered phospholipid vesicles, which are (ii) broken down by the addition of apoA-I at 37 °C, optionally additionally subjected to sonication, to form discoidal rHDL (Figure 3A<sub>I</sub>). Typically, the vesicles are produced by lipid film hydration or sonication methods or both. Alternatively, the lipid film can be hydrated with a buffer already containing apoA-I. The inclusion of exogenous amphiphiles, equipped with functional moieties or imaging labels, is relatively straightforward (Figure 3A<sub>II</sub>). It merely requires mixing them in at appropriate quantities, subsequently forming a lipid film that is hydrated with an apoA-I containing buffer. As a rule of thumb, low quantities (<2.5%) of exogenous amphiphiles can be easily incorporated, without affecting HDL's morphology, structural stability, or biological function.<sup>8</sup> The incorporation of exogenous amphiphiles in high quantities is required, for example, for Gd-DTPA labeled (phospho)lipids. This is related to MRI's relatively poor sensitivity to detecting exogenously administered contrast agents. We have shown the assembly of HDL with up to 33% Gd-DTPA-DSA (Gd-DTPA distearyl amide), albeit at the expense of contrast-generating and morphological properties.<sup>21</sup> Phospholipids that are head-group-functionalized with Gd-DTPA or Gd-DOTA are also available and tend to display physicochemical properties more closely related to ordinary phospholipids (we refer to section 5 for additional details).

### 3.2. Inclusion of Exogenous Compounds

Lipid film hydration methods also allow the inclusion of hydrophobic payloads (Figure 3A<sub>III</sub>), such as triglycerides or low-molecular weight hydrophobic drugs, as we have shown for simvastatin,<sup>14</sup> an LXR agonist,<sup>15</sup> and several other compounds. However, HDL's formation or stability may be negatively impacted by the core payload. We have observed that the inclusion of lysophospholipids,<sup>11</sup> with a relatively large hydrophilic fraction, forces the formation of small micelle-like structures that more stably encapsulate the core loading, which is further stabilized by the addition of apoA-I. Moreover, small quantities of cholesterol can be included to stabilize the supramolecular structure.

Small nanocrystals that are surface-coated with hydrophobic capping ligands can be incorporated in HDL nanobiologics (Figure 3A<sub>III</sub><sup>11</sup>). Unfortunately, lipid film hydration methods are suboptimal as they induce nanocrystal aggregation. We have developed alternative approaches in which phospholipids, typically a 1 to 1 mixture of ordinary and lysophospholipids, are mixed (in 10-fold excess) with the nanocrystals in nonpolar solvents. The resulting mixture is slowly dripped or infused in warm (~60 °C) buffer, resulting in instantaneous solvent evaporation and formation of micelles, some of which contain a single nanocrystal. Potential aggregates are removed, while gradient centrifugation methods can then be applied to purify the sample and remove empty micelles. Finally, apoA-I is added

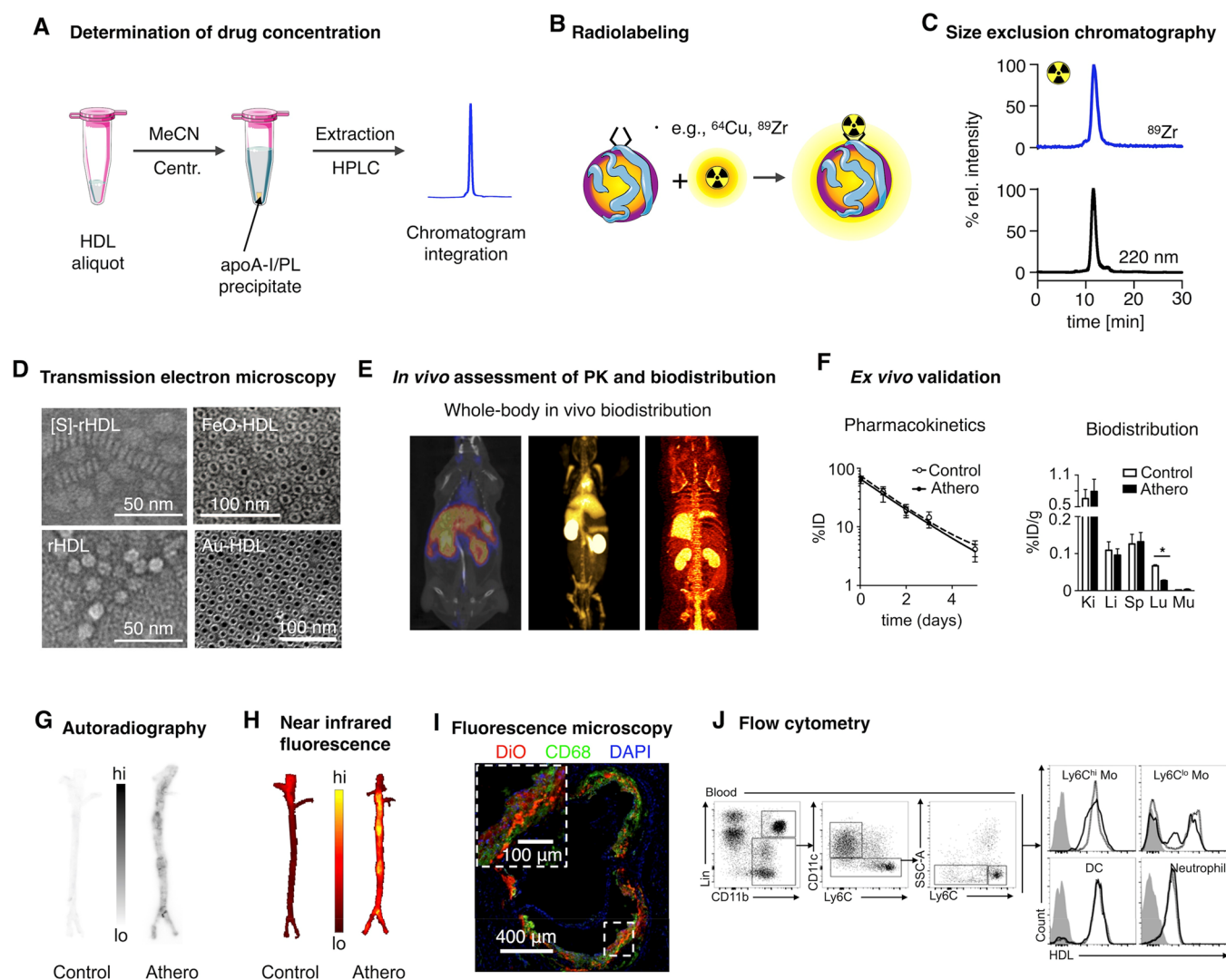


**Figure 4.** Characterization of HDL nanobiologics. (A) HDL drug content can be determined by HPLC. (B) Radiolabeling of HDL nanobiologics. (C) Size exclusion chromatography can be used to determine particle size and to confirm successful labeling of HDL and radiochemical purity. (D) Definitive size and morphology characterization should be performed by transmission electron microscopy. Reproduced with permission from refs 5, 11, and 14. Copyright 2013 and 2008 American Chemical Society, and 2014 Nature Publishing Group, respectively. (E) HDL labeling with positron emitters like  $^{89}\text{Zr}$  allows quantitative assessment of pharmacokinetics and biodistribution. (F) *Ex vivo* gamma counting and (G) autoradiography. Adapted with permission from ref 8. Copyright 2016 American College of Cardiology. (H) Evaluation of tissue distribution of HDL nanobiologics by NIRF imaging and cellular specificity by (I) fluorescence microscopy and (J) flow cytometry. Reproduced with permission from refs 14 and 8. Copyright 2014 Nature Publishing Group and 2016 American College of Cardiology, respectively.

to stabilize the structures and form nanocrystal-core HDL. The described infusion and dripping methods can also be applied to produce drug loaded HDL or HDL that contains functional amphiphiles, for therapeutic purposes but also to reroute HDL to alien targets, such as  $\alpha\beta_3$ -integrin expressed at the tumor vasculature<sup>22</sup> or collagen in atherosclerotic plaques.<sup>23</sup>

### 3.3. Scaling HDL Production

Most HDL nanobiologic technologies that we developed were applied for *in vitro* and mouse studies, requiring quantities that could be synthesized in a laboratory setting. Our desire to translate the technology to larger animal models required redesigning the production approach. First and foremost, large apoA-I quantities are necessary for HDL nanobiologic application (see section 2). Subsequent reconstitution of HDL requires a different approach from benchtop lipid-film hydration procedures. The approach we have implemented starts with the formation of a phospholipid suspension and the

hydrophobic payload, for example, simvastatin, in buffer containing apoA-I. The mixture, up to 1 L, is subsequently subjected to high-pressure homogenization, using a Microfluidizer high-shear fluid processor. The resulting HDL nanobiologics are physicochemically indiscernible from samples produced by regular benchtop methods.

### 3.4. Microfluidics-Based Production

HDL nanobiologics' fine-tuning is difficult to achieve using conventional benchtop methods, as they do not allow judiciously controlling minute compositional variations in a high-throughput manner. We recently developed a microfluidics approach that allows the instantaneous and continuous production of HDL nanobiologics,<sup>5,6</sup> containing surface payloads as well as core payloads, such as hydrophobic drugs, but also nanocrystals or polymers (Figure 3B<sub>1</sub>). Concurrently, we developed a fluorescence energy transfer microscopy technology to visualize HDL formation in a microfluidic chip,

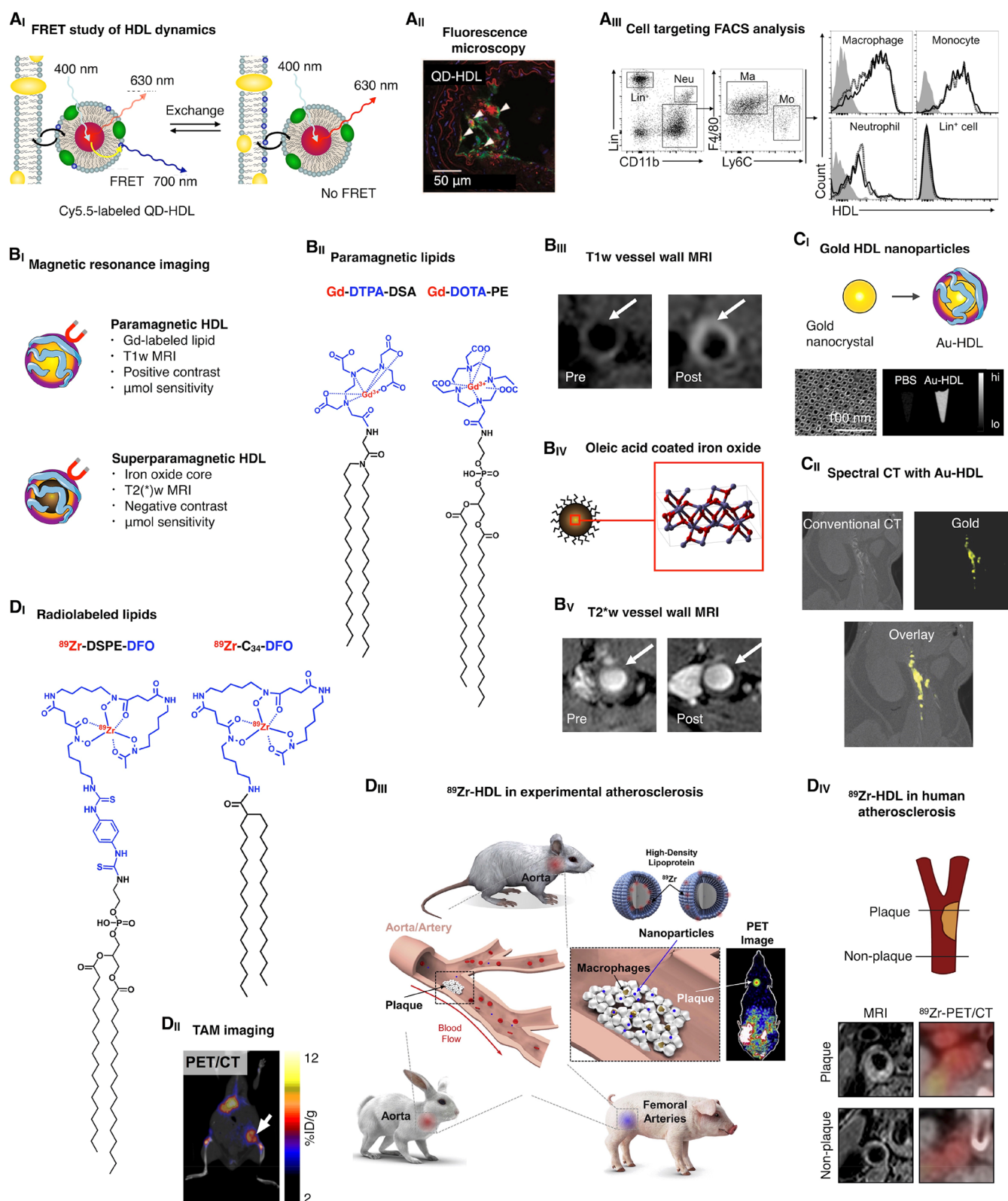


**Figure 5.** Imaging and HDL nanobiologics. (A<sub>i</sub>) Quantum dot-core HDL (QD-HDL) can be employed to study phospholipid exchange dynamics and cellular interactions by FRET. Reproduced with permission from ref 13. Copyright 2010 American Chemical Society. (A<sub>ii</sub>) QD-HDL can be visualized in target tissues by immunofluorescence. Reproduced with permission from ref 11. Copyright 2008 American Chemical Society. (A<sub>iii</sub>) Flow cytometric analyses allow the quantitative assessment of HDL nanobiologics' cellular specificity. Reproduced with permission from ref 8. Copyright 2016 American College of Cardiology. (B<sub>i</sub>) HDL nanobiologics that are MRI visible can be created by the inclusion of a high payload of (B<sub>ii</sub>) paramagnetic lipids, allowing (B<sub>iii</sub>) positive contrast MR imaging of vessel wall accumulation. Alternatively, superparamagnetic HDL nanobiologics can be constructed by the inclusion of (B<sub>iv</sub>) an iron oxide core, allowing (B<sub>v</sub>) negative contrast MR imaging of vessel wall accumulation. Reproduced with permission from ref 11. Copyright 2008 American Chemical Society. (C<sub>i</sub>) Similarly, gold nanocrystals can be incorporated in HDL, rendering electron dense Au-HDL nanobiologics that can be visualized by electron microscopy as well as CT imaging.

Figure 5. continued

Reproduced with permission from ref 5. Copyright 2013 American Chemical Society. (C<sub>II</sub>) Au-HDL accumulation in atherosclerotic plaque macrophages can be visualized in mice by spectral CT, a multicolor imaging technique. Reproduced with permission from ref 27. Copyright 2010 Radiological Society of North America. (D<sub>I</sub>) Lipids can be functionalized with DFO, a chelator that allows the complexation of <sup>89</sup>Zr, a radioisotope with a relatively long physical decay half-life, suitable for tracking long circulating HDL nanobiologics. We have studied the resulting <sup>89</sup>Zr-HDL's *in vivo* behavior and targeting potential by PET imaging, in (D<sub>II</sub>) a mouse tumor model, (D<sub>III</sub>) multiple atherosclerosis animal models, and even (D<sub>IV</sub>) cardiovascular patients. Reproduced with permission from refs 7 (D<sub>II</sub>), 31 (D<sub>III</sub>), and 30 (D<sub>IV</sub>). Copyright 2015 Society of Nuclear Medicine and Molecular Imaging, 2017 American College of Cardiology, and 2016 Elsevier, respectively.

in real time,<sup>24</sup> thus providing direct feedback on nanobiologic quality during its production (Figure 3B<sub>II</sub>). The inclusion of poly(lactic-co-glycolic acid) (PLGA) or poly(lactic acid) (PLA) polymers not only generates controlled release systems but also provides a polymeric core scaffold, whose size can be varied in a range of 50 nm up to 400 nm, onto which phospholipids and apoA-I can be templated, providing a platform for HDL nanobiologic size control.<sup>15</sup>

### 3.5. Library Approach

The microfluidics-facilitated ability to generate HDL mimetics with different shapes, sizes, compositions, and functions allowed us to establish a nanobiologic library<sup>15</sup> (Figure 3C). This library contains 10 nm HDL nanobiologics that are discoidal when reconstituted from phospholipids and apoA-I. Spherical HDL, in the size range of 20 to 30 nm, can be generated by the inclusion of triglycerides, while polymer core nanobiologics' sizes can be precisely varied from 40 to 150 nm, and up to 400 nm. Imaging labels, including fluorescent dyes and radioisotopes, can be straightforwardly integrated, allowing HDL nanobiologics' *in vitro* and *in vivo* screening using optical methods, like flow cytometry or near-infrared fluorescence (NIRF) imaging, and nuclear imaging, respectively. HDL nanobiologics' characterization and *in vivo* screening are discussed in sections 4 and 6, respectively.

## 4. CHARACTERIZATION

### 4.1. Physicochemical Properties

First quality control characterization of HDL nanoparticles deals with composition, size, and morphology. As mentioned in section 2, typical reconstitution methods comprise several purification steps that may lead to substantial loss of material. Therefore, it is imperative to assess the final chemical composition of the sample. Several phosphorus/choline (e.g., Rouser assay) and protein (e.g., Bradford assay) quantification methods can be used to determine phospholipid and apoA-I content, respectively. Determination of load concentration depends on its chemical nature. Small molecule drugs can be extracted from HDL using water-miscible organic solvents (typically acetonitrile), and their concentration can be established by high-performance liquid chromatography (HPLC) (Figure 4A). Inorganic loads, that is, iron oxide or gold, can be determined by inductively coupled plasma mass spectrometry (ICP-MS). Size can be measured by dynamic light scattering (DLS), which derives a hydrodynamic diameter from particle motion characteristics. From these measurements, a polydispersity index (PDI) can also be obtained, providing information on size heterogeneity. Depending on the load, rHDLs can measure from 8 to 9 nm (nanodiscs) to 400 nm (polymer-loaded nanoparticles<sup>15</sup>), with PDIs in the 0.1–0.3 range. The use of SEC can complement DLS analyses by clearly identifying different size populations or enabling detection of small molecular impurities. SEC is the ideal method to prove

that certain labels are loaded on HDL. For instance, we have developed radiolabeling strategies for rHDL nanoparticles<sup>7</sup> (Figure 4B, see also section 5.1). After purification, we conduct a quality control SEC to demonstrate coelution of radioactivity with the nanobiologics and to determine radiochemical purity (Figure 4C). However, the gold standard to establish size and morphology is transmission electron microscopy (TEM, Figure 4D). Nanocrystal-core HDL nanoparticles clearly show the dense inorganic core surrounded by a “halo” of lipids and apoA-I (Figure 4D, right). These core-loaded particles are spherical, whereas TEM images of nonloaded HDL or HDL loaded with small molecule drugs show the typical stacking of nanodiscs (Figure 4D, left).

### 4.2. Biological Features

The modifications introduced in the reconstitution/loading process may alter HDL's biological activity. A simple way to assess if its activity is retained is by evaluating the nanoparticles' ability to efflux cholesterol from loaded cells.<sup>15</sup> The assay uses tritiated (<sup>3</sup>H-labeled) cholesterol and radioactivity counting for this purpose. The modifications described in this Account have little or no effect on cholesterol efflux capacity. ApoA-I/HDL also promotes cholesterol esterification, and this process can also be tested to probe biological activity. Another feature that can be compromised is the capacity to interact with apoA-I targets via its native receptors. As already mentioned, HDL displays a preferential affinity for myeloid cells through ABCA1, ABCG1, and SR-BI receptors. How these interactions are preserved for different HDL nanobiologics has not been fully studied, but flow cytometry assays can be deployed to evaluate if their affinity for these immune cells has been altered.<sup>15</sup> We do, however, observe that nanobiologics significantly larger than native HDL display a different tissue distribution signature, with increased accumulation in hematopoietic organs such as the spleen.<sup>15</sup>

### 4.3. In Vivo Behavior

Molecular imaging techniques offer attractive ways to study nanomaterials' *in vivo* behavior. However, no standalone imaging technique brings together the necessary spatial/temporal resolution, sensitivity, or tissue penetration to provide information at whole-body, tissue, and cellular level. For HDL nanobiologics, we have developed labeling strategies that enable fluorescence- and positron emission-based imaging in different animals and disease contexts.<sup>7,8,15</sup> Zirconium-89 (<sup>89</sup>Zr)-labeling allows not only the *in vivo* visualization and quantification of radioactivity distribution by PET (Figure 4E) but also the corroboration of the results by *ex vivo* gamma counting (Figure 4F). Moreover, PET imaging can be performed dynamically and longitudinally to derive *in vivo* pharmacokinetic data,<sup>8</sup> while *ex vivo* autoradiography provides valuable information about regional distribution in a given tissue (Figure 4G). Similarly, fluorescently labeled HDL allows NIRF imaging *in vivo* and *ex vivo* (Figure 4H). Cellular distribution in tissues of interest can

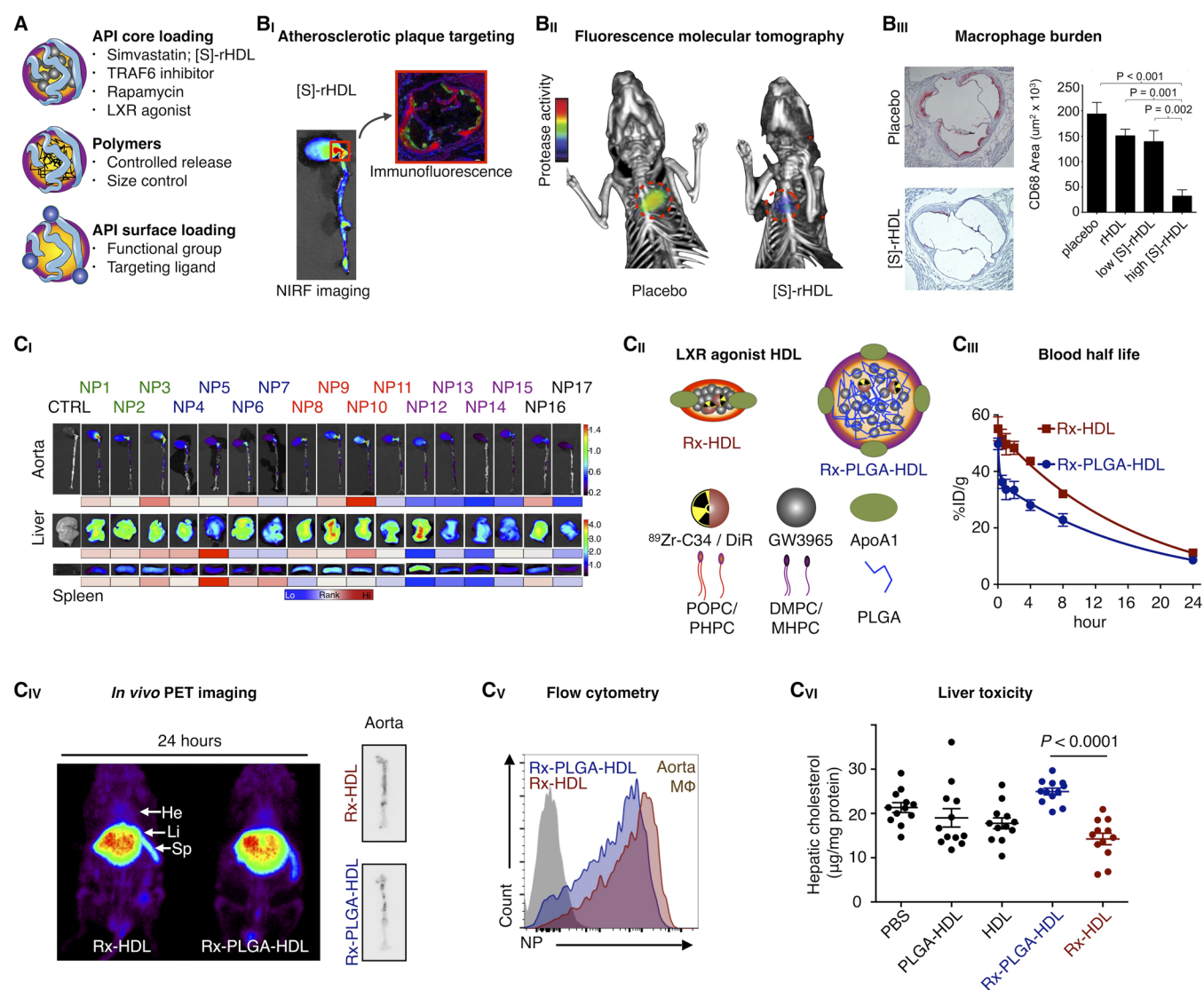


**Figure 6.** Immunotherapy with HDL nanobiologics. (A) HDL nanobiologics suitable for immunotherapy can include therapeutically active payloads or controlled release polymers in the core or compounds can be integrated in the corona. (B<sub>i</sub>) Simvastatin-loaded HDL nanobiologics ([S]-rHDL) accumulate in atherosclerotic plaques in mice, as observed by NIRF imaging of excised aortas and immunofluorescence. (B<sub>ii</sub>) A [S]-rHDL treatment regimen consisting of 4 intravenous doses in 1 week, drastically reduces vessel wall inflammation in atherosclerotic mice, as quantified by FMT/CT imaging, (B<sub>iii</sub>) corresponding with a > 80% macrophage burden reduction. Reproduced with permission from ref 14. Copyright 2014 Nature Publishing Group. (C<sub>i</sub>) The HDL nanobiologic library presented in Figure 3C was screened in atherosclerotic mice. Accumulation in the aorta and target organs at 24 h post-intravenous administration is shown. In addition, the library's pharmacokinetics and immune cell specificity was investigated. (C<sub>ii</sub>) An LXR agonist was incorporated in two selected HDL nanobiologics, with very diverse *in vivo* properties, rendering Rx-HDL and Rx-PLGA-HDL. (C<sub>iii</sub>) Blood half-lives, (C<sub>iv</sub>) biodistribution, atherosclerotic plaque targeting, and (C<sub>v</sub>) plaque macrophage specificity were established from <sup>89</sup>Zr-labeled Rx-HDL and Rx-PLGA-HDL. (C<sub>vi</sub>) The Rx-PLGA-HDL nanobiologic, which accumulates in the liver more pronouncedly, generated liver toxicity, while for the Rx-HDL nanobiologic liver toxicity was abolished. Reproduced with permission from ref 15. Copyright 2016 National Academy of Sciences of the United States of America.

be probed by high-resolution confocal microscopy (Figure 4I), whereas flow cytometric analysis can be used to obtain quantitative and detailed information about cellular uptake (Figure 4J).

## 5. DIAGNOSTICS

### 5.1. Imaging Modalities and Labels

We have shown that HDL nanobiologics can be modified for their visualization using different imaging techniques, namely, optical imaging<sup>9,11,13</sup> (Figure 5A), MRI<sup>9–12,18,25,26</sup> (Figure 5B), CT<sup>11,27</sup> (Figure 5C), and PET<sup>7,8</sup> (Figure 5D). Each modality has its own strengths.<sup>28</sup> While optical methods have excellent

spatial resolution and allow multiplex imaging, nuclear imaging techniques excel in sensitivity. CT and MRI exhibit good spatial resolution, with the latter displaying excellent soft tissue contrast, which allows delineation of small structures like the aortic vessel wall. Each modality requires the incorporation of a label to generate the imaging signal or contrast, and these labels fall into two main groups:

**5.1.1. Lipophilic Molecules.** Commercially available hydrophobic dyes can be easily incorporated into HDL nanobiologics during the reconstitution process. Similarly, HDL-based MRI contrast agents can be generated from hydrophobic paramagnetic molecules containing gadolinium-

(III) chelates<sup>18</sup> (Figure 5B<sub>I</sub>) that can also be purchased from specialized vendors. To enable radiolabeling of HDL's cargo with <sup>89</sup>Zr, we have developed lipophilic deferoxamine B (DFO) derivatives<sup>15,29</sup> (Figure 5D<sub>I</sub>). Additionally, HDL nanobiologics can be labeled through covalent modification of apoA-I with fluorescent dyes or DFO.<sup>8</sup>

**5.1.2. Nanocrystals.** Another way to generate contrast is by including a nanocrystal core. Thus far, we have produced iron oxide<sup>5,11</sup> (Figure 5B<sub>III</sub>), gold<sup>5,11,27</sup> (Figure 5C<sub>I</sub>), and quantum dot-loaded<sup>5,11</sup> HDL for MRI, CT, and optical imaging purposes, respectively. These nanobiologics are spherical, measuring approximately 10 nm, and retain HDL's biological features.

## 5.2. Applications

Fluorescently labeled HDL can be used to study nanoparticle dynamics by Förster Resonance Energy Transfer (FRET) (Figure 5A<sub>I</sub>). As HDL's components may behave differentially, incorporation of two fluorophores with overlapping absorption/emission spectra can be exploited to determine whether the nanoparticle components remain together after administration.<sup>13</sup> Fluorescent HDL can also be used for confocal microscopy to determine distribution with (sub)cellular resolution<sup>11</sup> (Figure 5A<sub>II</sub>), while flow cytometry allows assessing cell subsets<sup>8,15</sup> (Figure 5A<sub>III</sub>). HDL nanobiologics can be used as contrast agent for vessel wall imaging with MRI (Figure 5B<sub>I</sub>). Modification with paramagnetic lipids (Figure 5B<sub>II</sub>) generates T1-MRI contrast agents (Figure 5B<sub>III</sub>), whereas core loading with small superparamagnetic iron oxide nanocrystals<sup>5,11</sup> (Figure 5B<sub>IV</sub>) yields T2(\*)-MRI contrast agents (Figure 5B<sub>V</sub>). However, MRI contrast sensitivity is low (micromolar range) and requires large amounts of contrast agents to be injected, compromising translation. The same applies for gold nanocrystal-loaded HDL (Au-HDL) (Figure 5C<sub>I</sub>). At high doses (500 mg/kg), Au-HDL accumulation in atherosclerotic lesions of *ApoE*<sup>-/-</sup> mice could be visualized by CT<sup>27</sup> (Figure 5C<sub>II</sub>). More recently, we have developed strategies to radiolabel HDL nanobiologics with <sup>89</sup>Zr, including the use of hydrophobic DFO derivatives<sup>7,8,15</sup> (Figure 5D<sub>I</sub>). <sup>89</sup>Zr-HDL was used to image tumor-associated macrophages in a mouse model of breast cancer by PET<sup>7</sup> (Figure 5D<sub>II</sub>). The same HDL nanobiologics were tested in a translational study that included *in vivo* evaluation in three animal models of atherosclerosis, using PET/CT and PET/MRI<sup>8</sup> (Figure 5D<sub>III</sub>). This radiolabeling strategy has been taken all the way to humans to assess HDL accumulation in carotid lesions by PET/CT<sup>30</sup> (Figure 5D<sub>IV</sub>).

## 6. IMMUNOTHERAPY WITH NANOBIOLOGICS

Epidemiological studies on patient lipid profiles have identified high HDL levels, or to be more precise a favorable HDL to LDL ratio, to negatively correlate with the occurrence of coronary artery disease and cardiovascular events.<sup>32</sup> This observation sparked the cardiovascular research community to investigate HDL's atheroprotective function and its potential use as an injectable therapy.<sup>33</sup> Preclinically, HDL-induced atherosclerosis regression was observed in rabbits<sup>34</sup> and mice.<sup>35</sup> Unfortunately, clinical trials have not (or have marginally) shown benefits of exogenously administered HDL for cardiovascular patients. For example, in a randomized trial, conducted at 51 centers in the USA, The Netherlands, Canada, and France, no reduction in coronary atherosclerosis was observed in patients that received infusions of the HDL

mimetic CER-001.<sup>36</sup> At the same time, we have shown (Figure 5D<sub>IV</sub>) that radiolabeled CER-001 accumulates in atherosclerotic plaques of patients.<sup>30</sup> Hence, HDL itself may not display atheroregressive properties in human subjects, but the ability to target plaque macrophages renders it suitable for drug delivery purposes, at relatively low apoA-I doses.

### 6.1. Inclusion of Drugs

The integration of therapeutically active molecules in HDL can be achieved through different routes. Naturally, microRNAs are transported in plasma by HDL. This endogenous concept is mimicked by Shad Thaxton's group; his team has shown the exploitation of HDL nanostructures for short interfering RNA delivery for the treatment of cancer in multiple reports.<sup>37</sup> Alternatively, therapeutic payloads can be incorporated in HDL's surface, for example, through conjugation with phospholipids or cholesterol or by their linking to apoA-I. We have primarily focused on the inclusion of hydrophobic compounds, especially low molecular weight drugs, in HDL's lipophilic core. This approach was established to be very useful for certain drugs, with inclusion efficiencies of more than 50%.<sup>14,15</sup> Moreover, we developed strategies to increase a drug's compatibility with a given nanodelivery vehicle,<sup>38</sup> increasing HDL's scope for targeted therapy purposes.

### 6.2. Nanobiologic Immunotherapy

As the HDL nanobiologic platform technology (Figure 6A) is designed to inherently interact with immune cells, primarily myeloid cells, it is very well-suited for targeted immunotherapy.<sup>15</sup> In a series of studies, we have thoroughly explored nanobiologic immunotherapy in atherosclerosis mouse models.<sup>14,15,39</sup> We found that simvastatin-loaded HDL ([S]-rHDL) targets atherosclerotic plaque macrophages<sup>14</sup> (Figure 6B<sub>I</sub>). A treatment regimen consisting of 4 intravenous injections in a timespan of 1 week reduced atherosclerotic plaque protease activity, an inflammation measure, by approximately 65%, as determined by *in vivo* fluorescence molecular tomography imaging (Figure 6B<sub>II</sub>). Quantitative histology revealed that this corresponded with a > 80% reduction in macrophage burden (Figure 6B<sub>III</sub>). In an ensuing study, we found that the rapidly induced plaque inflammation reduction could be sustained with concomitant oral statin therapy.<sup>39</sup>

The library technology introduced in section 3 is of particular interest for the design and development of targeted immunotherapies. Extensive screening in an atherosclerosis mouse model revealed differential behavior of HDL nanobiologics within the library, specifically in relation to their biodistribution and plaque targeting efficiency (Figure 6C<sub>I</sub>), as well as relative immune cell specificity. From this screen, we identified two HDL nanobiologics with vastly different *in vivo* properties, one of which targets plaque macrophages efficiently (Rx-HDL), while the other pronouncedly accumulates in the liver (Rx-PLGA-HDL). We then selected GW3965, a liver X receptor agonist that failed translation due to liver toxicity, and incorporated it into these two HDL nanobiologics (Figure 6C<sub>II</sub>). In addition to differences in pharmacokinetics (Figure 6C<sub>III</sub>), we also observed subtle differences in liver and atherosclerotic plaque accumulation (Figure 6C<sub>IV</sub>), as well as macrophage affinity (Figure 6C<sub>V</sub>). Importantly, GW3965's liver toxicity was augmented by Rx-PLGA-HDL but significantly lessened by Rx-HDL (Figure 6C<sub>VI</sub>), while preserving therapeutic function and the ability to decrease cholesterol accumulation in immune cells. This study highlights the

importance of *in vivo* screening and rational (and data driven) optimization of nanoimmunotherapies.

## 7. CONCLUSION AND OUTLOOK

In the past decade and a half, we have established nanobiologic platform technology based on HDL. The versatility and modularity of this platform allow the creation of HDL nanobiologics that can be detected by nuclear and optical methods,<sup>13,14</sup> as well as multiple clinically relevant imaging techniques, including PET,<sup>7,8</sup> CT,<sup>11,27</sup> and MRI.<sup>9,11,18</sup> Not only does this allow HDL tracking, but at the same time, the diagnostically active nanobiologics can be employed for molecular imaging purposes.<sup>28</sup> In addition to its inherent targets, we have been able to reroute HDL to collagen and the tumor vasculature, by the surface conjugation of ligands.<sup>22,23</sup> Importantly, HDL library technology<sup>5,6,15</sup> allows establishing nanobiologic immunotherapies with inherent affinity for myeloid cells, at the target site, but also in the hematopoietic organs.

Although this Account focused on our developments and vision, we would like to acknowledge others who made tangible contributions to this field. Gang Zheng and Jerry Glickson have done seminal work in the application of LDL in cancer models.<sup>40</sup> Nucleic acid delivery with (gold core) HDL was pioneered by Shad Thaxton,<sup>37</sup> while David Cormode developed gold-core HDL for multicolor CT molecular imaging purposes.<sup>27</sup> Many others have made important contributions as well.<sup>41</sup>

Looking forward, we are focused on developing novel technologies to improve HDL nanobiologics' drug loading and targeting capabilities, we are expanding HDL nanobiologics' use to a variety of inflammatory diseases and refocusing the platform's imaging capabilities to assist in the design of targeted immunotherapies. Finally, in addition to escalating HDL nanobiologics' evaluation to large animal models,<sup>8</sup> we have ventured into performing human studies with radiolabeled HDL,<sup>30</sup> but our overarching goal is to translate HDL nanobiologic immunotherapies to the clinic.

## AUTHOR INFORMATION

### Corresponding Authors

\*Willem J. M. Mulder. E-mail: [willem.mulder@mssm.edu](mailto:willem.mulder@mssm.edu).

\*Carlos Pérez-Medina. E-mail: [carlos.perez-medina@mountsinai.org](mailto:carlos.perez-medina@mountsinai.org).

### ORCID

Willem J. M. Mulder: 0000-0001-8665-3878

### Notes

The authors declare no competing financial interest.

### Biographies

**Willem J. M. Mulder**, Ph.D., is a Professor at Mount Sinai's Translational and Molecular Imaging Institute (TMII) in New York and at the Academic Medical Center (AMC) of the University of Amsterdam. His research focuses on the development of HDL nanobiologics and their application for precision imaging and targeted therapy in cardiovascular disease and cancer.

**Mandy M. T. van Leent**, M.D., is a postdoctoral fellow at TMII.

**Marnix Lameijer** is a Ph.D. student at the AMC.

**Edward A. Fisher**, M.D., Ph.D., is Professor of Cardiovascular Medicine at NYU.

**Zahi A. Fayad**, Ph.D., is Professor of Radiology and Medicine and director of TMII.

**Carlos Pérez Medina**, Ph.D., is an Assistant Professor at TMII. His research focuses on radiotracer design and the development of nanoparticle radiolabeling strategies for nuclear imaging.

## ACKNOWLEDGMENTS

This work was supported by National Institutes of Health Grants R01HL118440, R01HL125703, and P01HL131478, a Netherlands Organisation for Scientific Research Vidi (all to W.J.M.M.), and Grants R01EB009638 and P01HL131478 (to Z.A.F.).

## REFERENCES

- (1) EL Andaloussi, S.; Mäger, I.; Breakefield, X. O.; Wood, M. J. A. Extracellular Vesicles: Biology and Emerging Therapeutic Opportunities. *Nat. Rev. Drug Discovery* **2013**, *12* (5), 347–357.
- (2) Segrest, J. P.; Jones, M. K.; De Loof, H.; Brouillette, C. G.; Venkatachalapathi, Y. V.; Anantharamaiah, G. M. The Amphipathic Helix in the Exchangeable Apolipoproteins: A Review of Secondary Structure and Function. *J. Lipid Res.* **1992**, *33* (2), 141–166.
- (3) Havel, R. J.; Eder, H. A.; Bragdon, J. H. The Distribution and Chemical Composition of Ultracentrifugally Separated Lipoproteins in Human Serum. *J. Clin. Invest.* **1955**, *34* (9), 1345–1353.
- (4) Rothblat, G. H.; Phillips, M. C. High-Density Lipoprotein Heterogeneity and Function in Reverse Cholesterol Transport. *Curr. Opin. Lipidol.* **2010**, *21*, 229.
- (5) Kim, Y.; Fay, F.; Cormode, D. P.; Sanchez-Gaytan, B. L.; Tang, J.; Hennessy, E. J.; Ma, M.; Moore, K.; Farokhzad, O. C.; Fisher, E. A.; Mulder, W. J. M.; Langer, R.; Fayad, Z. A. Single Step Reconstitution of Multifunctional High-Density Lipoprotein-Derived Nanomaterials Using Microfluidics. *ACS Nano* **2013**, *7* (11), 9975–9983.
- (6) Sanchez-Gaytan, B. L.; Fay, F.; Lobatto, M. E.; Tang, J.; Ouimet, M.; Kim, Y.; van der Staay, S. E. M.; van Rijs, S. M.; Priem, B.; Zhang, L.; Fisher, E. A.; Moore, K. J.; Langer, R.; Fayad, Z. A.; Mulder, W. J. M. HDL-Mimetic PLGA Nanoparticle to Target Atherosclerosis Plaque Macrophages. *Bioconjugate Chem.* **2015**, *26* (3), 443–451.
- (7) Perez-Medina, C.; Tang, J.; Abdel-Atti, D.; Hogstad, B.; Merad, M.; Fisher, E. A.; Fayad, Z. A.; Lewis, J. S.; Mulder, W. J. M.; Reiner, T. PET Imaging of Tumor-Associated Macrophages with <sup>89</sup>Zr-Labeled High-Density Lipoprotein Nanoparticles. *J. Nucl. Med.* **2015**, *56* (8), 1272–1277.
- (8) Pérez-Medina, C.; Binderup, T.; Lobatto, M. E.; Tang, J.; Calcagno, C.; Giesen, L.; Wessel, C. H.; Witjes, J.; Ishino, S.; Baxter, S.; Zhao, Y.; Ramachandran, S.; Eldib, M.; Sánchez-Gaytán, B. L.; Robson, P. M.; Bini, J.; Granada, J. F.; Fish, K. M.; Stroes, E. S. G.; Duivenvoorden, R.; Tsimikas, S.; Lewis, J. S.; Reiner, T.; Fuster, V.; Kjær, A.; Fisher, E. A.; Fayad, Z. A.; Mulder, W. J. M. In Vivo PET Imaging of HDL in Multiple Atherosclerosis Models. *JACC Cardiovasc. Imaging* **2016**, *9*, 950.
- (9) Frias, J. C.; Williams, K. J.; Fisher, E. A.; Fayad, Z. A. Recombinant HDL-Like Nanoparticles: A Specific Contrast Agent for MRI of Atherosclerotic Plaques. *J. Am. Chem. Soc.* **2004**, *126* (50), 16316–16317.
- (10) Cormode, D. P.; Briley-Saebo, K. C.; Mulder, W. J. M.; Aguinaldo, J. G. S.; Barazza, A.; Ma, Y.; Fisher, E. A.; Fayad, Z. A. An ApoA-I Mimetic Peptide High-Density-Lipoprotein-Based MRI Contrast Agent for Atherosclerotic Plaque Composition Detection. *Small* **2008**, *4* (9), 1437–1444.
- (11) Cormode, D. P.; Skajaa, T.; van Schooneveld, M. M.; Koole, R.; Jarzyna, P.; Lobatto, M. E.; Calcagno, C.; Barazza, A.; Gordon, R. E.; Zanonico, P.; Fisher, E. A.; Fayad, Z. A.; Mulder, W. J. M. Nanocrystal Core High-Density Lipoproteins: A Multimodality Contrast Agent Platform. *Nano Lett.* **2008**, *8* (11), 3715–3723.
- (12) Skajaa, T.; Cormode, D. P.; Jarzyna, P. A.; Delshad, A.; Blachford, C.; Barazza, A.; Fisher, E. A.; Gordon, R. E.; Fayad, Z. A.; Mulder, W. J. M. The Biological Properties of Iron Oxide Core High-

Density Lipoprotein in Experimental Atherosclerosis. *Biomaterials* **2011**, *32* (1), 206–213.

(13) Skajaa, T.; Zhao, Y.; van den Heuvel, D. J.; Gerritsen, H. C.; Cormode, D. P.; Koole, R.; van Schooneveld, M. M.; Post, J. A.; Fisher, E. A.; Fayad, Z. A.; de Mello Donega, C.; Meijerink, A.; Mulder, W. J. M. Quantum Dot and Cy5.5 Labeled Nanoparticles to Investigate Lipoprotein Biointeractions via Förster Resonance Energy Transfer. *Nano Lett.* **2010**, *10*, 5131.

(14) Duivenvoorden, R.; Tang, J.; Cormode, D. P.; Mieszawska, A. J.; Izquierdo-Garcia, D.; Ozcan, C.; Otten, M. J.; Zaidi, N.; Lobatto, M. E.; van Rijs, S. M.; Priem, B.; Kuan, E. L.; Martel, C.; Hewing, B.; Sager, H.; Nahrendorf, M.; Randolph, G. J.; Stroes, E. S. G.; Fuster, V.; Fisher, E. A.; Fayad, Z. A.; Mulder, W. J. M. A Statin-Loaded Reconstituted High-Density Lipoprotein Nanoparticle Inhibits Atherosclerotic Plaque Inflammation. *Nat. Commun.* **2014**, *5*, 3065.

(15) Tang, J.; Baxter, S.; Menon, A.; Alaarg, A.; Sanchez-Gaytan, B. L.; Fay, F.; Zhao, Y.; Ouimet, M.; Braza, M. S.; Longo, V. A.; Abdel-Atti, D.; Duivenvoorden, R.; Calcagno, C.; Storm, G.; Tsimikas, S.; Moore, K. J.; Swirski, F. K.; Nahrendorf, M.; Fisher, E. A.; Pérez-Medina, C.; Fayad, Z. A.; Reiner, T.; Mulder, W. J. M. Immune Cell Screening of a Nanoparticle Library Improves Atherosclerosis Therapy. *Proc. Natl. Acad. Sci. U. S. A.* **2016**, *113* (44), E6731–E6740.

(16) Bricarello, D. A.; Smilowitz, J. T.; Zivkovic, A. M.; German, J. B.; Parikh, A. N. Reconstituted Lipoprotein: A Versatile Class of Biologically-Inspired Nanostructures. *ACS Nano* **2011**, *5* (1), 42–57.

(17) Segrest, J. P.; Garber, D. W.; Brouillette, C. G.; Harvey, S. C.; Anantharamaiah, G. M. The Amphipathic  $\alpha$  Helix: A Multifunctional Structural Motif in Plasma Apolipoproteins. *Adv. Protein Chem.* **1994**, *45*, 303–369.

(18) Cormode, D. P.; Chandrasekar, R.; Delshad, A.; Briley-Saebo, K. C.; Calcagno, C.; Barazza, A.; Mulder, W. J. M.; Fisher, E. A.; Fayad, Z. A. Comparison of Synthetic High Density Lipoprotein (HDL) Contrast Agents for MR Imaging of Atherosclerosis. *Bioconjugate Chem.* **2009**, *20* (5), 937–943.

(19) Ryan, R. O.; Forte, T. M.; Oda, M. N. Optimized Bacterial Expression of Human Apolipoprotein A-I. *Protein Expression Purif.* **2003**, *27* (1), 98–103.

(20) Tardy, C.; Goffinet, M.; Boubekeur, N.; Ackermann, R.; Sy, G.; Bluteau, A.; Cholez, G.; Keyserling, C.; Lalwani, N.; Paolini, J. F.; Dasseux, J.-L.; Barbaras, R.; Baron, R. CER-001, a HDL-Mimetic, Stimulates the Reverse Lipid Transport and Atherosclerosis Regression in High Cholesterol Diet-Fed LDL-Receptor Deficient Mice. *Atherosclerosis* **2014**, *232* (1), 110–118.

(21) Ramos-Cabrer, P.; Fay, F.; Sanchez-Gaytan, B. L.; Tang, J.; Castillo, J.; Fayad, Z. A.; Mulder, W. J. M. Conformational Changes in High-Density Lipoprotein Nanoparticles Induced by High Payloads of Paramagnetic Lipids. *ACS Omega* **2016**, *1* (3), 470–475.

(22) Chen, W.; Jarzyna, P. A.; van Tilborg, G. A. F.; Nguyen, V. A.; Cormode, D. P.; Klink, A.; Griffioen, A. W.; Randolph, G. J.; Fisher, E. A.; Mulder, W. J. M.; Fayad, Z. A. RGD Peptide Functionalized and Reconstituted High-Density Lipoprotein Nanoparticles as a Versatile and Multimodal Tumor Targeting Molecular Imaging Probe. *FASEB J.* **2010**, *24* (6), 1689–1699.

(23) Chen, W.; Cormode, D. P.; Vengrenyuk, Y.; Herranz, B.; Feig, J. E.; Klink, A.; Mulder, W. J. M.; Fisher, E. A.; Fayad, Z. A. Collagen-Specific Peptide Conjugated HDL Nanoparticles as MRI Contrast Agent to Evaluate Compositional Changes in Atherosclerotic Plaque Regression. *JACC Cardiovasc. Imaging* **2013**, *6* (3), 373–384.

(24) Sanchez-Gaytan, B. L.; Fay, F.; Hak, S.; Alaarg, A.; Fayad, Z. A.; Pérez-Medina, C.; Mulder, W. J. M.; Zhao, Y. Real-Time Monitoring of Nanoparticle Formation by FRET Imaging. *Angew. Chem., Int. Ed.* **2017**, *56* (11), 2923–2926.

(25) Frias, J. C.; Ma, Y.; Williams, K. J.; Fayad, Z. A.; Fisher, E. A. Properties of a Versatile Nanoparticle Platform Contrast Agent To Image and Characterize Atherosclerotic Plaques by Magnetic Resonance Imaging. *Nano Lett.* **2006**, *6* (10), 2220–2224.

(26) Barazza, A.; Blachford, C.; Even-Or, O.; Joaquin, V. A.; Briley-Saebo, K. C.; Chen, W.; Jiang, X.-C.; Mulder, W. J. M.; Cormode, D. P.; Fayad, Z. A.; Fisher, E. A. The Complex Fate in Plasma of

Gadolinium Incorporated into High-Density Lipoproteins Used for Magnetic Imaging of Atherosclerotic Plaques. *Bioconjugate Chem.* **2013**, *24* (6), 1039–1048.

(27) Cormode, D. P.; Roessl, E.; Thran, A.; Skajaa, T.; Gordon, R. E.; Schlomka, J.-P.; Fuster, V.; Fisher, E. A.; Mulder, W. J. M.; Proksa, R.; Fayad, Z. A. Atherosclerotic Plaque Composition: Analysis with Multicolor CT and Targeted Gold Nanoparticles. *Radiology* **2010**, *256* (3), 774–782.

(28) Mulder, W. J. M.; Jaffer, F. A.; Fayad, Z. A.; Nahrendorf, M. Imaging and Nanomedicine in Inflammatory Atherosclerosis. *Sci. Transl. Med.* **2014**, *6* (239), 239sr1.

(29) Perez-Medina, C.; Abdel-Atti, D.; Zhang, Y.; Longo, V. A.; Irwin, C. P.; Binderup, T.; Ruiz-Cabello, J.; Fayad, Z. A.; Lewis, J. S.; Mulder, W. J. M.; Reiner, T. A Modular Labeling Strategy for In Vivo PET and Near-Infrared Fluorescence Imaging of Nanoparticle Tumor Targeting. *J. Nucl. Med.* **2014**, *55* (10), 1706–1711.

(30) Zheng, K. H.; van der Valk, F. M.; Smits, L. P.; Sandberg, M.; Dasseux, J.-L.; Baron, R.; Barbaras, R.; Keyserling, C.; Coolen, B. F.; Nederveen, A. J.; Verberne, H. J.; Nell, T. E.; Vugts, D. J.; Duivenvoorden, R.; Fayad, Z. A.; Mulder, W. J. M.; van Dongen, G. A. M. S.; Stroes, E. S. G. HDL Mimetic CER-001 Targets Atherosclerotic Plaques in Patients. *Atherosclerosis* **2016**, *251*, 381–388.

(31) Leeper, N. J.; Park, S.; Smith, B. R. High-Density Lipoprotein Nanoparticle Imaging in Atherosclerotic Vascular Disease. *JACC Basic to Transl. Sci.* **2017**, *2* (1), 98–100.

(32) Desforges, J. F.; Rifkind, B. M.; Gordon, D. J. High-Density Lipoprotein—the Clinical Implications of Recent Studies. *N. Engl. J. Med.* **1989**, *321* (19), 1311–1316.

(33) Kingwell, B. A.; Chapman, M. J.; Kontush, A.; Miller, N. E. HDL-Targeted Therapies: Progress, Failures and Future. *Nat. Rev. Drug Discovery* **2014**, *13* (6), 445–464.

(34) Badimon, J. J.; Badimon, L.; Fuster, V. Regression of Atherosclerotic Lesions by High Density Lipoprotein Plasma Fraction in the Cholesterol-Fed Rabbit. *J. Clin. Invest.* **1990**, *85* (4), 1234–1241.

(35) Feig, J. E.; Rong, J. X.; Shamir, R.; Sanson, M.; Vengrenyuk, Y.; Liu, J.; Rayner, K.; Moore, K.; Garabedian, M.; Fisher, E. A. HDL Promotes Rapid Atherosclerosis Regression in Mice and Alters Inflammatory Properties of Plaque Monocyte-Derived Cells. *Proc. Natl. Acad. Sci. U. S. A.* **2011**, *108* (17), 7166–7171.

(36) Fogelman, A. M. Trying to Harness the Potential of HDL: Wishful Thinking or Sound Strategy? *Eur. Heart J.* **2014**, *35* (46), 3248–3249.

(37) McMahon, K. M.; Thaxton, C. S. High-Density Lipoproteins for the Systemic Delivery of Short Interfering RNA. *Expert Opin. Drug Delivery* **2014**, *11* (2), 231–247.

(38) Zhao, Y.; Fay, F.; Hak, S.; Manuel Perez-Aguilar, J.; Sanchez-Gaytan, B. L.; Goode, B.; Duivenvoorden, R.; de Lange Davies, C.; Bjørkøy, A.; Weinstein, H.; Fayad, Z. A.; Pérez-Medina, C.; Mulder, W. J. M. Augmenting Drug-carrier Compatibility Improves Tumour Nanotherapy Efficacy. *Nat. Commun.* **2016**, *7*, 11221.

(39) Tang, J.; Lobatto, M. E.; Hassing, L.; van der Staay, S.; van Rijs, S. M.; Calcagno, C.; Braza, M. S.; Baxter, S.; Fay, F.; Sanchez-Gaytan, B. L.; Duivenvoorden, R.; Sager, H. B.; Astudillo, Y. M.; Leong, W.; Ramachandran, S.; Storm, G.; Perez-Medina, C.; Reiner, T.; Cormode, D. P.; Strijkers, G. J.; Stroes, E. S. G.; Swirski, F. K.; Nahrendorf, M.; Fisher, E. A.; Fayad, Z. A.; Mulder, W. J. M. Inhibiting Macrophage Proliferation Suppresses Atherosclerotic Plaque Inflammation. *Sci. Adv.* **2015**, *1* (3), e1400223–e1400223.

(40) Zheng, G.; Chen, J.; Li, H.; Glickson, J. D. Rerouting Lipoprotein Nanoparticles to Selected Alternate Receptors for the Targeted Delivery of Cancer Diagnostic and Therapeutic Agents. *Proc. Natl. Acad. Sci. U. S. A.* **2005**, *102* (49), 17757–17762.

(41) Denisov, I. G.; Sligar, S. G. Nanodiscs in Membrane Biochemistry and Biophysics. *Chem. Rev.* **2017**, *117* (6), 4669–4713.